Thermal Unfolding of Yeast Glycine Transfer RNA†

C. W. Hilbers,* G. T. Robillard, R. G. Shulman,
R. D. Blake, P. K. Webb, R. Fresco, and D. Riesner

ABSTRACT: In the present investigations the molecular unfolding of yeast $tRNA^{Gly}$ has been studied by a combination of nuclear magnetic resonance spectroscopy, melting techniques, and relaxation kinetics. From these studies the following pathway of unfolding was found. In a coupled melting transition the tertiary, the DHU, and the anticodon structure are disrupted. This is followed by the melting of the acceptor arm, while the TψC arm, which only contains G·C pairs, melts out last. Interestingly, during the first melting transition a new structure not belonging to the original cloverleaf structure is formed. The thermodynamic and kinetic parameters of the melting transitions were determined and are discussed in relation to earlier work. The present nuclear magnetic resonance (NMR) experiments as well as earlier studies show that the ring current calculations based on the cloverleaf structure provide a good first-order interpretation of the NMR spectra of tRNA.

Recent high-resolution nuclear magnetic resonance (NMR) studies of the hydrogen-bonded ring NH protons in base pairs of nucleic acids have shown that these resonances are shifted to very low fields so that they are well separated from the majority of the proton resonances and very often are well resolved.

The resonance positions have been explained by assuming that in the absence of interactions with neighbors the ring N hydrogen-bonded protons of the A·U pairs are found near −14.6 ppm and those of the G·C pairs near −13.6 ppm (Shulman et al., 1973). Resonances are then shifted to higher fields by the ring currents from neighboring bases stacked above and below. With parameters for these two interactions fixed it has been possible to calculate spectra which agree with the observed to within 0.3 ppm. Hence, certain well-resolved resonances can be assigned merely by comparing the calculated and observed spectra. However, for the majority of the resonances which are not so well resolved, definitive assignments to particular base-paired protons have been made by comparing the calculated spectra with the changes which occur upon heating the tRNA solutions, since it has been observed that the resonances from a particular helical arm generally disappear together in a restricted temperature interval (Crothers et al., 1973, 1974; Hilbers and Shulman, 1974). The same conclusion was drawn from optical melting experiments (Römer et al., 1969). In this way the problem of using the calculated positions to assign resonances is reduced from one with about 20 resonances to one with about five resonances, which is more accurately solved.

Recently, it has been shown for the case of *Escherichia coli* $tRNA^{fMet}$ how the NMR "melting" measurements in conjunction with temperature jump relaxation studies can be used to determine the sequence of melting of different parts of the tRNA molecule (Crothers et al., 1974). This was accomplished by mapping the observed and assigned NMR transitions, with their limited kinetic information, onto particular relaxations which trace out the temperature dependence of the kinetics. In this way a rather complete and detailed picture of the path of unfolding and folding of this macromolecule with the associated kinetic and thermodynamic parameters has been obtained. A detailed knowledge of the energy contents of the different structural parts of tRNA molecules is essential for the interpretation of the microscopic events, which occur during the interaction of tRNA molecules with their cognate synthetases and with the ribosomes in the course of protein synthesis. In addition this information may lead to an understanding of the inherent physical parameters, which predetermine some tRNA species to function in other processes, e.g. gene regulation.

In the present paper the NMR "melting" and temperature jump relaxation measurements, made upon samples of yeast $tRNA^{Gly}$, are discussed. Some of the hydrogen-bonded proton resonances disappear because they broaden when the proton lifetime becomes shorter than ~5 ms during melting, and others disappear by an equilibrium process in which the helical population decreases (Crothers et al., 1973). In the latter case, which is reported here for the first time, the line widths do not change as the peak intensities decrease, in perfect accord with the temperature jump measurements. In addition, the temperature-dependent NMR spectra show the formation of a "new structure" during the melting of yeast $tRNA^{Gly}$, a phenomenon which has not been observed before.

Methods

The yeast $tRNA^{Gly}$ spectra from the 0.15 M KCl solution were obtained with a Bruker 270-MHz spectrometer. The spectra consist of 75 accumulations each of 50 s, run in the frequency sweep mode. Spectra from the other samples were obtained on a Varian 300-MHz spectrometer. The spectra were accumulated in a Nicolet 1024 channel analyzer. Each spectrum consists of 60 scans of 100 s each unless specified otherwise. The solute conditions are given in the figure captions.

Fast kinetic measurements were carried out in an improved version (Coutts et al., 1974) of the Eigen/de Maeyer

† From the Department of Biophysical Chemistry, University of Nijmegen, Nijmegen, The Netherlands (C.W.H.), Department of Physical Chemistry, University of Groningen, Groningen, The Netherlands (G.T.R.), Bell Laboratories, Murray Hill, New Jersey 07974 (R.G.S.), Department of Biochemistry, Princeton University, Princeton, New Jersey 08540 (R.D.B., P.K.W., R.F.), and Medizinische Hochschule, Institut für Klinische Biochemie und Physiologische Chemie, Hannover, West Germany (D.R.). *Received August 14, 1975.*

Table I: Areas[a] of the Resonances from Yeast $tRNA^{Gly}$ Dissolved in a 0.15 M KCl Solution.

	Protons											
	A	B	C	D	E	F	G	H	I	J	K	L	M
Temp. (°C)	1.5[b]	2	1		15			2	1.5				1
15	0.19	0.25	0.14		1.74			0.23	0.17	0.52	0.30	0.20	0.10
20	0.18	0.27	0.14		1.80			0.21	0.16	0.46	0.29	0.17	0.09
25	0.15	0.24	0.13		1.68			0.16	0.10	0.43	0.26	0.14	0.07
30	0.09	0.20	0.09		1.48			0.08	0.04	0.54		0.10	0.04
35	0.04	0.15	0.02		1.46								
40		0.16			1.68								
45		0.19			1.58								
50		0.18			1.49								
55		0.16			1.33								
60		0.12			1.01								

[a] Areas, representing line intensities, are given in arbitrary units; 1 proton corresponds to 0.12 unit. [b] The numbers given just below the letters are the number of protons at 15 °C. The numbers are discussed in the text.

temperature-jump apparatus (Eigen and de Maeyer, 1963). The absorbance changes were monitored at 260 and 280 nm. The numerical analysis has been carried out by graphical methods. The reversibility of the investigated transitions was checked after each series of experiments in order to rule out errors due to possible degradation during the experiments.

Results

(A) *The NMR Spectra.* NMR spectra of yeast $tRNA^{Gly}$ were recorded at three different salt conditions, i.e. in 0.15 M KCl with no Mg^{2+}, in 1.0 M NaCl with no Mg^{2+}, and in 0.1 M NaCl with 0.01 M $MgCl_2$, as a function of temperature. Figure 1 shows the 270-MHz spectra of the 0.15 M KCl solution. As is usually observed under low salt conditions the NMR spectra change over a wide temperature range. To help follow these changes the resonances in Figure 1 are lettered. Because of the good resolution we were able to determine the relative intensities of different special features (Table I). On the assumption that in the 20 °C spectrum the resonance H corresponds to two protons, the lowest field resonance A has an intensity of 1.5 protons, the resonance B of slightly more than 2 protons, and the resonance C slightly more than 1 proton. The block of resonances between −13.5 ppm and −12 ppm corresponds to 15 protons, while peak I has an intensity of 1.5 protons. Thus, there is a total of about 24 protons in the spectral region of −15 to −11 ppm. The assignment of an intensity of two protons to the resonance H was based on the following reasoning. The signal appears like two partially resolved resonances. Taking resonance H as corresponding to two protons results in an intensity close to two protons for resonance B, while C has slightly more and M has slightly less intensity than unity. We could have chosen resonance A or I as corresponding to one proton, but then it would have been difficult to assign integer values to the other resonances, while in addition the spectra recorded at different salt conditions show that resonance A splits into two resonances and the intensity of I is highly variable (see Figures 2 and 3). Earlier studies suggested that the region from −15 ppm to −11.5 ppm contained only hydrogen-bonded proton resonances from secondary structure base pairs in the cloverleaf (Lightfoot et al., 1973). However, more recent experiments have proven that the region between −15 and −11 ppm contains resonances of hydrogen-bonded protons involved in tertiary structure (Hilbers and Shulman, 1974; Reid et al., 1975; Wong and Kearns, 1974; Robillard et al., 1976). The present results also agree with these observations, since there is an intensity of 24 protons between −15 and −11 ppm, while only 20 are expected from the cloverleaf model (cf. Figure 5). Moreover, in the region of −11 to −9 ppm the ring N protons of G·U pairs (Robillard et al., 1976) and additional tertiary structure resonances are observed.

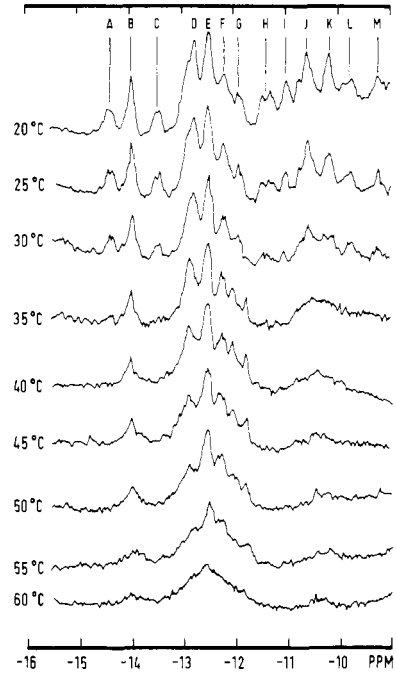

FIGURE 1: Spectra (270 MHz) of yeast $tRNA^{Gly}$ as a function of temperature. Each spectrum consists of 75 accumulations in a time average computer: sample volume 0.15 ml, [yeast $tRNA^{Gly}$] = 2 mM, [KCl] = 0.15 M, no Mg^{2+}, [cacodylate buffer] = 0.01 M, pH 7. The horizontal scale gives the position in parts per million (ppm) downfield from sodium 4,4-dimethyl-4-silapentanesulfonate (DSS).

The temperature dependence of the spectra of yeast $tRNA^{Gly}$ dissolved in a 1.0 M NaCl solution is shown in Figure 2. Because of good resolution we chose the 42 °C spectrum to determine the relative intensities of the differ-

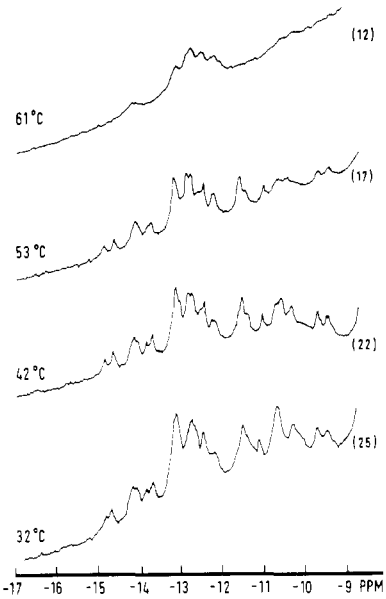

FIGURE 2: Spectra (300 MHz) of yeast $tRNA^{Gly}$ as a function of temperature. Solution conditions: [yeast $tRNA^{Gly}$] = 2 mM, [NaCl] = 1.0 M, [cacodylate buffer] = 0.01 M, no Mg^{2+}, pH 7. The numbers at the right-hand side of the spectra indicate the integrated spectral area between −15 and −11 ppm expressed in numbers of protons.

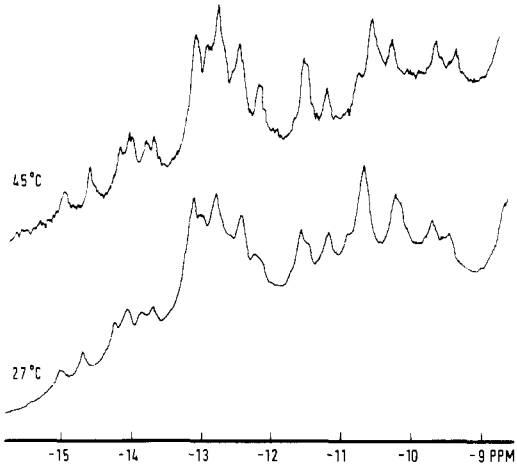

FIGURE 3: Spectrum (300 MHz) of yeast $tRNA^{Gly}$ at 27 and 45 °C. Solution conditions: [yeast $tRNA^{Gly}$] = 2 mM, [NaCl] = 0.01 M, [cacodylate buffer] = 0.01 M, [$MgCl_2$] = 0.01 M.

ent resonances. On the basis of setting the integrated intensity between −13.5 and −12 ppm equal to 15 protons we find again close to 5 protons in the region of −15 to −13.5 ppm. In this region the two peaks near −14.7 ppm (corresponding to peak A in Figure 1) have again an integrated intensity of about 1.5 protons. In the 0.15 M KCl solution these resonances coincide. The resonance at −11.5 ppm, corresponding to peak H in Figure 1, now has an intensity of 3 protons, which is also suggested by its form.

The spectra obtained in the Mg^{2+} containing solution (Figure 3) do not significantly differ from those taken in 1.0 M NaCl, although small differences can be observed. For instance the splitting of the low-field resonance around −14.7 ppm is even more pronounced than in the 1.0 M NaCl solution. The spectra of the Mg^{2+} containing solution recorded at 27 and 42 °C are virtually identical. The spectrum at 42 °C is somewhat better resolved and also some resonances appear slightly shifted with respect to the 27 °C spectrum.

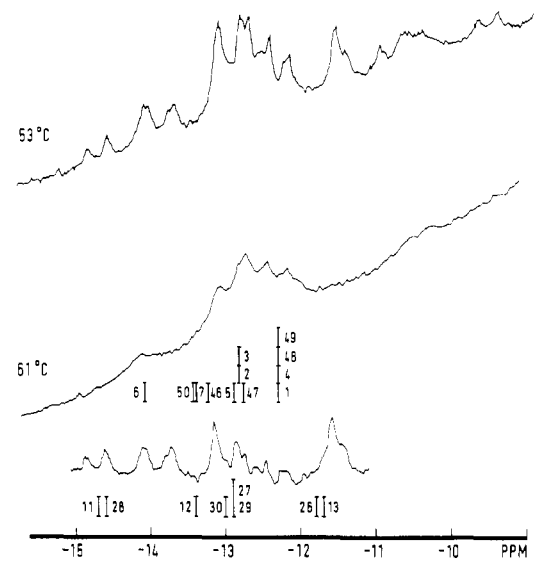

FIGURE 4: Spectra (300 MHz) of yeast $tRNA^{Gly}$ at 53 and 61 °C together with their difference spectrum. The solution conditions are as indicated below Figure 2. The stick spectrum below the difference spectrum was calculated for the DHU and anticodon stem on the basis of ring-current parameters given by Shulman et al. (1973). The stick spectrum just below the 61 °C spectrum was calculated for the acceptor and TψC stem with these ring current parameters.

On the basis of the spectral assignments later in this section the spectra have been simulated (see Figure 8). The results are in good agreement with the intensity considerations presented above.

(B) *Temperature Dependence of the NMR Spectra.* Sequential melting of the tRNA facilitates the assignment of particular resonances to certain protons in the molecule. Examination of Figures 1 and 2 shows that sequential melting does indeed take place.

We first examine the temperature dependence of the spectra of the 1.0 M NaCl solution (Figure 2). When the temperature is raised from 32 to 53 °C there is a loss of integrated intensity as indicated on the right-hand side of Figure 2. Between 53 and 61 °C the spectrum drastically changes shape and the intensity drops to ~12 protons. These two spectra are shown separately in Figure 4 along with their difference spectrum. Our interpretation of the differences between the 53 and 61 °C spectra is that the resonances of the DHU- and anticodon helices and of the tertiary structure are lost by 61 °C. The loss of resonances from the two helices is seen from a comparison of the 53 to 61 °C difference spectrum with the lowest stick spectrum in Figure 4. The stick spectrum was calculated for the DHU and anticodon helices on the basis of the ring current shift parameters presented previously (Shulman et al., 1973) using the cloverleaf model shown in Figure 5 (Yoshida, 1973).

The well-resolved resonances below −13.5 ppm and the resonance near −11.5 ppm serve as markers for the interpretation. The loss of the resonances near −11.5 ppm agrees very well with the calculated positions of pairs A·ψ-13 and G·C-26, since no other resonances were calculated or observed to be within 0.5 ppm. Similarly the loss of all but one resonance below −13.5 ppm can be explained as the disappearance of A·U-11, A·U-28, and A·U-12 from the DHU and anticodon arms. The broad single resonance, which persists at 61 °C, is assigned on this basis to A·U-6. To complete the assignment we suggest that A·U-28 is real-

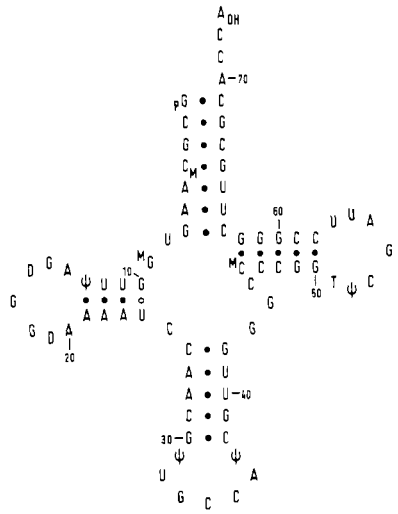

FIGURE 5: Cloverleaf sequence of yeast $tRNA^{Gly}$ as determined by Yoshida (1973).

Table II: Comparison between Calculated and Observed[a] Resonance Positions of the Individual Base Pairs of the Cloverleaf of Yeast $tRNA^{Gly}$.

Base Pair	Calcd Position	Obs Position	$\delta_{obsd} - \delta_{calcd}$
1 G·C	−12.3 (1.2)	−12.5	−0.2
2 C·G	−12.8	−12.8	0
3 G·C	−12.8	−12.8	0
4 C_m·G	−12.3	−12.35	−0.05
5 A·U	−12.9	−12.8	+0.1
6 A·U	−14.1	−14.2	−0.1
7 G·C	−13.4 (0.2)	−13.1	+0.3
11 U·A	−14.7	−14.6	+0.1
12 U·A	−13.5	−13.7	−0.2
13 ψ·A	−11.5 (0.7)	−11.55	−0.05
26 C·G	−11.8 (0.7)	−11.7	+0.1
27 A·U	−12.9	−12.95	−0.05
28 A·U	−14.6	−14.2	+0.4
29 C·G	−12.9	−13.05	−0.15
30 G·C	−12.9 (0.1)	−12.7	+0.2
46 C·G	−13.3 (0.2)	−13.2	+0.1
47 C·G	−12.8	−12.7	+0.1
48 C·G	−12.3	−12.45	−0.15
49 G·C	−12.3	−12.18	+0.12
50 G·C	−13.4 (0.1)	−13.1	+0.3

[a] The observed positions were deduced from the experiments in the 0.15 M KCl solution. The numbers in parentheses indicate shift contributions from neighboring bases adjacent to the double helical region, assuming that these residues are stacked in a regular helical fashion.

ly observed at −14.1 ppm and A·U-12 at −13.7 ppm as given in Table II, which compares the calculated positions with those obtained from the experimental assignments. Moreover, we suggest that the lowest field resonance near −14.8 ppm comes from a tertiary structure hydrogen-bonded proton, because of the sensitivity of its position to ionic strength and the absence and or presence of Mg^{2+} ions (Figures 1–3). The difference spectrum (in Figure 4) shows the loss of three resonances in the region around −12.9 ppm, whose positions are very close to the positions calculated for A·U-27, G·C-29, and G·C-30.

Figure 2 shows that the intensity loss, which is particularly manifest between 53 and 61 °C for the resonances

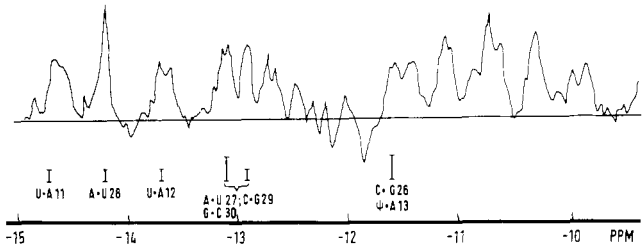

FIGURE 6: The difference spectrum of the 20 °C minus the 35 °C spectrum given in Figure 1. The stick spectra are the line positions of the peaks of the difference spectrum given in Figure 4.

below −13.5 ppm and at −11.5 ppm, had started already between 32 and 53 °C. It is noteworthy that these resonances decrease in intensity without broadening or shifting. The most likely explanation of this kind of behavior is a slow equilibrium between two states, the base-paired and the non-base-paired state where only the base-paired state is being observed. This will be discussed in more detail below.

The temperature dependence of the yeast $tRNA^{Gly}$ spectra from the 0.15 M KCl solution is shown in Figure 1. There are no detectable changes between 15 and 20 °C, but above 20 °C the intensities begin to decrease (see Table I).

The "melting" proceeds analogously to that observed for the 1.0 M NaCl solution (Figure 2). The lowest (A, B, and C) and high field (H and I) resonances lose intensity without shifting and broadening (Figure 1). Peak A is not appreciably split under these conditions although there is a slight broadening suggesting the splitting. By 35 or 40 °C intensities corresponding to one proton have disappeared from peaks A, B, C, I, L, and M, while peak H has lost the equivalent of two protons. The difference spectrum (Figure 6) between 20 and 35 °C shows these losses, as well as indicating where intensity is lost from the central region of the spectrum. It is important to note that the stick diagram, for which we took observed positions as assigned in the difference spectrum in Figure 4, fits very well the observed difference spectrum in Figure 6. Only some slight shifts are seen around −13.0 ppm. However, as expected, in 0.15 M KCl the transition temperature is considerably lower than in the 1.0 M NaCl solution (~35 °C compared to ~55 °C). It was mentioned above that between 20 and 35 °C the resonance intensities decrease while the widths remain constant. This can be seen most clearly in lines A, C, H, and I. If these intensities are determined by a slow equilibrium between two states, then the dissociation equilibrium constants can be determined from the measured intensities at different temperatures:

$$K_D = (I_0 - I)/I$$

where I is the intensity from the residual intact molecules and I_0 is the intensity when all molecules are intact. This has been done and the derived values of K_D are plotted in Figure 7. For comparison the figure also shows as a solid line the values of K_D derived from the optical measurements in the temperature range.

It is of interest to note that at ~35 °C a new sharp resonance appears between peak G and H with an intensity of about one proton (see Figure 1). The appearance of this resonance occurs simultaneously with an increase in integrated intensity which is particularly pronounced when proceeding from 35 to 40 °C (see Table I under DEFG). Since this resonance is so narrow and the total spectrum does not broad-

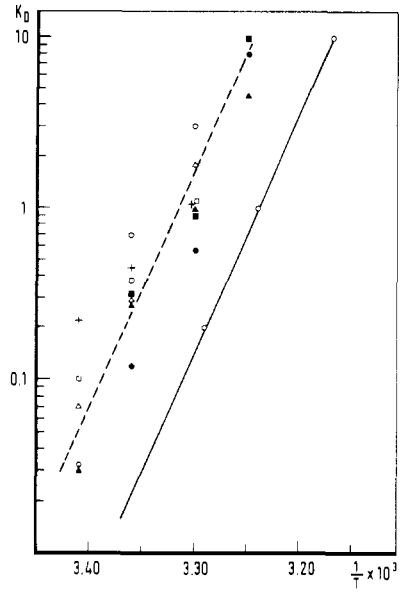

FIGURE 7: The dissociation equilibrium constant of the low-temperature melting transition observed by NMR in the 0.15 M KCl solution as a function of temperature. The solid line gives the equilibrium constants for the same process calculated from the optical differential melting curve (Figure 11).

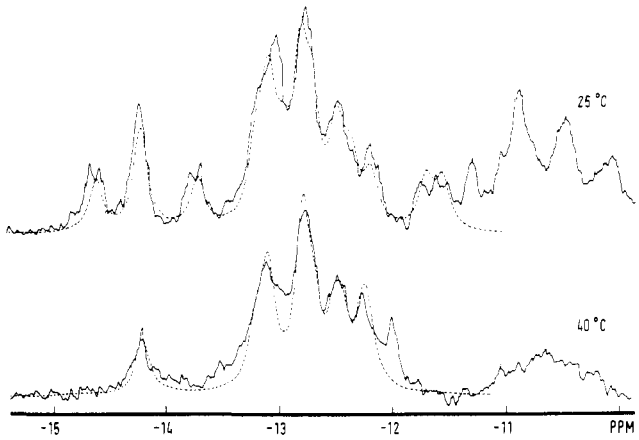

FIGURE 8: Experimental and computer-simulated 270-MHz spectra of yeast $tRNA^{Gly}$. The solid lines represent the experimental spectra. The dashed lines are the computer-simulated spectra. The solution conditions are given in the caption for Figure 1.

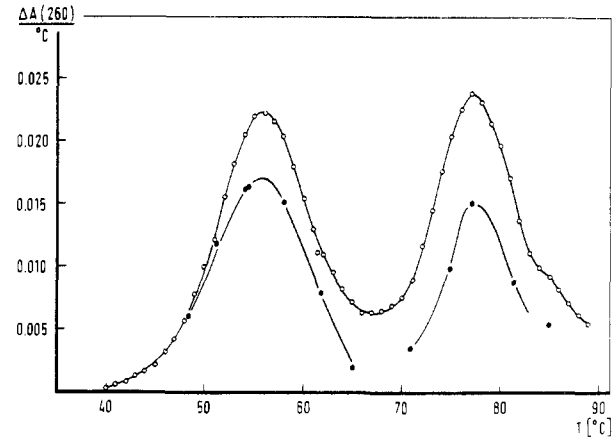

FIGURE 9: Differential melting curve (○) and temperature-jump amplitudes (●) of $tRNA^{Gly}$ at 260 nm in 0.01 M sodium cacodylate–1.0 M Na^+–10^{-4} M EDTA (pH 7.0). The total temperature-jump amplitudes including the unresolvable fast stacking equilibrium agree within the limits of error with the equilibrium measurements and are not depicted in the figure. The vertical scale refers to a concentration of 1 A_{260} unit at 20 °C.

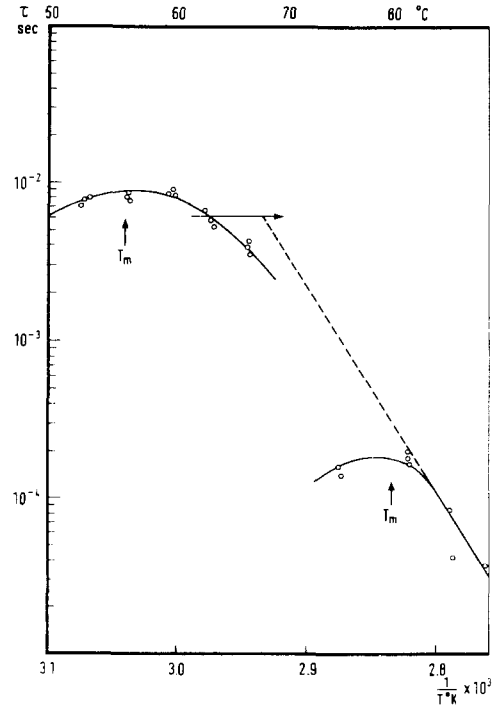

FIGURE 10: Plot of the change of the relaxation times of yeast $tRNA^{Gly}$ with temperature. Solution conditions are given in the caption for Figure 9. The vertical arrows indicate the melting temperatures of the individual transition. The dashed line, representing $1/k_d$, has been drawn through the high temperature τ values and 2τ at $T = T_m$. It has been extrapolated to the temperature where the helix lifetime is 5 ms. The bar at the 5-ms level indicates the temperature region in which a significant broadening is observed of the resonances of the acceptor and TψC stem.

en this increase in intensity cannot come from dimerization or aggregation of the tRNA molecules. Instead, it is attributed to the formation of a new structure developing from the melted DHU, anticodon and tertiary structure. In addition to this new, well-resolved resonance, a second resonance appears at about 13.0 ppm as can be seen by an increase in the height of the trough at about 13.0 ppm, this being compatible with the integrated intensity of this region (Table I) since there are 12.6 protons in the region D, E, F, G at 35 °C and 14.6 protons at 40 °C.

As the temperature is raised past 45 °C the resonances definitely broaden indicating the melting of the acceptor and TψC stem and of the newly formed structure. This is seen most clearly in the lowest field resonance and the new resonance between G and H.

Starting from the ring current calculated positions of the acceptor- and TψC arm resonances (Table II) the NMR spectrum of this part of the tRNA molecule was computer simulated. Slight shifts from the calculated positions had to be introduced to fit the experimental spectrum (see Table II). Except for the extra resonance at −12 ppm and a difference in intensity around −13 ppm the agreement is very good (Figure 8). The extra intensity is due to the newly formed resonances, which have just been discussed. Subsequently the 25 °C spectrum was simulated by adding to the 40 °C simulated spectrum the resonances of the anticodon and the DHU arm for which the positions were taken from

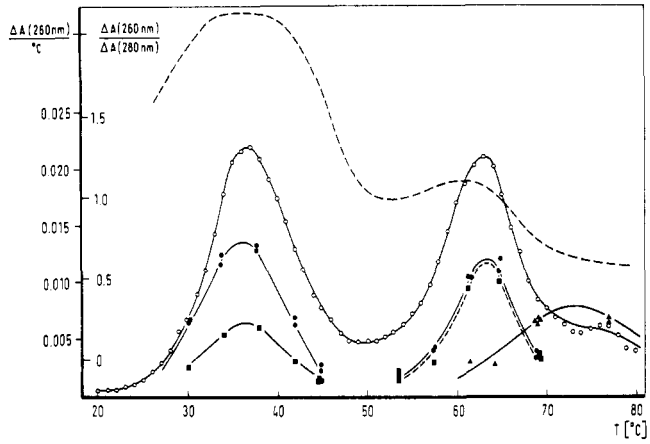

FIGURE 11: Differential melting curve and temperature-jump amplitudes of $tRNA^{Gly}$ in 0.01 M sodium cacodylate–0.15 M Na^+–10^{-4} M EDTA (pH 7.0): differential melting curve at 260 nm (○); ratios $\Delta A(260\text{ nm})/\Delta A(280\text{ nm})$ as determined from melting curves (- - -); temperature-jump amplitudes of the resolved relaxation effects at 260 nm (●) and 280 nm (■ and ▲), respectively; otherwise see Figure 9.

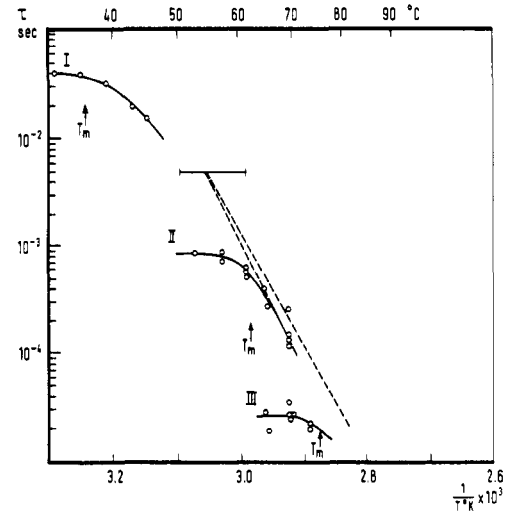

FIGURE 12: Plot of the change of the relaxation times of yeast $tRNA^{Gly}$ with temperature. Solution conditions are given in the caption for Figure 11. The dashed lines, representing $1/k_d$, were drawn through 2τ at $T = T_m$ and through the high-temperature values of τ in the case of transition II. The choice of the slope of the line connected with transition III is explained in the text. The lines are extrapolated to the temperature where the helix lifetime is 5 ms. The bar at the 5 ms level indicates the temperature region in which a significant broadening of the resonances of the acceptor and TψC arm is observed.

the difference spectrum given in Figure 6. To this end the 40 °C position of the pair G·C-4 had to be slightly moved to higher field. Again reasonable agreement between the simulated and observed spectrum is obtained (Figure 8). The standard deviation of the calculated vs. experimental positions was found to be 0.17 ppm, which includes the contributions of base pairs at the ends of the double helical regions.

(C) *Optical Experiments.* Both temperature-jump and the differential melting experiments were carried out on 0.15 M NaCl and 1.0 M NaCl solutions of yeast $tRNA^{Gly}$ containing no Mg^{2+}.

The differential melting curves from the 1.0 M NaCl solution are shown in Figure 9. Two well-resolved transitions are observed, characterized by melting temperatures (T_m) of 57 and 81 °C. A third transition at even higher temperatures could not be followed completely. In the temperature-jump experiments both these transitions could be characterized by a single relaxation time, the relaxation time of the low-temperature transition being in the millisecond range and the higher temperature transition in the range of 10^{-4} s; their temperature dependence is plotted in Figure 10. In addition to the equilibrium melting curves the amplitudes of the relaxation processes are plotted in Figure 9. The positions of the transitions measured by kinetic and equilibrium methods are in good agreement.

In 0.15 M NaCl the melting transitions are shifted to lower temperature with respect to those obtained in the 1.0 M NaCl solution, i.e. the first transition is shifted from 57 to 36 °C while the second is shifted from 81 to 67 °C. In the low salt sample the third transition is observed with a T_m of 76 °C (see Figure 11). The relaxation times are given in Figure 12. Changing the solution conditions does not fundamentally change the kinetics in accordance with earlier experiences (Römer and Riesner, 1973).

From the differential melting curves and from the temperature-jump amplitudes the reaction enthalpies were calculated; they are given in Table III.

(D) *Combination of Optical and NMR Melting.* The melting of the present tRNA structure appears as two different phenomena in the NMR spectra. The disrupture of the anticodon stem, the DHU stem, and the tertiary structure, associated with the low-temperature transition, appears as a loss of resonance intensity, while no broadening is observed. The dissociation of the acceptor and TψC stem shows up via the lifetime broadening effect of the hydrogen-bonded ring N protons in the high-temperature transition. Previously it has been discussed how the latter "NMR melting" can be mapped onto the relaxation experiments (Crothers et al., 1974) and this is demonstrated in Figures 10 and 12. Briefly, on the basis that NMR line broadening will only be observed when the helix lifetime is about 5 ms (Crothers et al., 1973, 1974) in Figures 10 and 12 temperature regions in which the helix lifetime is ~5 ms have been indicated by bars. Since on the high-temperature side of a particular transition, the relaxation time τ is dominated by the helix dissociation constant, and making use of the fact that at T_m, $2\tau = (k_d)^{-1}$, a line can be drawn through the high-temperature points of the τ curve and the point 2τ at T_m. This line should intersect the bar at the 5-ms level obtained from NMR, as is indeed found in Figures 10 and 12.

In the 0.15 M KCl solution this intersection yields a temperature of ~55 °C at which the helix lifetime is 5 ms for both high-temperature transitions (Figure 12). The line drawn for the highest temperature transition, T_m = 72 °C,

Table III: Thermodynamic Parameters of the Melting Transitions of Yeast $tRNA^{Gly}$.

Transition	Structural Region	T_m (°C) 0.15 M	T_m (°C) 1.0 M	ΔH (kcal/mol) 0.15 M	ΔH (kcal/mol) 1.0 M
	Tertiary interaction DHU arm				
I	Anticodon arm	36	56	65	74
	Intermediate structure formed				
II	Acceptor arm + intermediate structure	67	81	90	104
III	TψC arm	76		55	

needs some explanation since no tangent can be drawn to the τ values at the high-temperature side of the relaxation curve. In addition to the point $2\tau = (k_d)^{-1}$ at T_m we need the slope of the line. This was calculated by equating the dissociation activation enthalpy to the reaction enthalpy, the latter being obtained from the differential melting curve and the temperature-jump amplitudes. The justification for this procedure is given in the Discussion section. The combination of NMR and temperature-jump experiments did not allow us to assign a particular relaxation curve to the melting of either the acceptor or the TψC stem. This had to come from the wavelength dependence of the optical melting experiments which is represented in Figure 11 by the ratios $\Delta A(260\text{ nm})/\Delta A(280\text{ nm})$. The value of 0.6 can only be interpreted as the melting of G·C pairs, showing that the highest temperature transition is due to a helix containing only G·C pairs, which links it to the melting of the TψC stem.

In the 1 M NaCl solution the 5-ms helix lifetime of the high-temperature transition is according to the temperature-jump result predicted to be at 68 °C in good agreement with expectation from NMR.

The low-temperature melting transition in 0.15 M KCl observed in NMR between 25 and 40 °C was assigned to the melting of the DHU stem and the anticodon stem and to the disrupture of the tertiary structure. The melting is characterized by a loss of intensity of the NMR lines without broadening taking place. Such a behavior is to be expected when there is a shift of the equilibrium helix → coil, while the double helix has a long lifetime compared to the reciprocal of the line widths observed for the hydrogen-bonded protons. On the basis of this consideration one predicts the lifetime of the helix to be longer than 5 ms during this melting process. This is observed indeed in the temperature-jump experiments (Figure 12, transition I).

From the decrease of intensity of the NMR lines the dissociation equilibrium constant (K_D) has been calculated for the individual resonances and plotted as a function of temperature together with the equilibrium constants obtained from the differential melting curve (Figure 7). The discrepancy between these results does not arise from the different methods applied. In both experiments the same ionic strength was used; in the NMR experiments it was adjusted by dialyzing against a 0.15 M KCl solution, while in the optical experiments this was done against a 0.15 M NaCl solution. At the time of the experiments we did not know that sodium and potassium ions influence the thermal stability differently. In the meantime, however, Urbanke et al. (1975) found that sodium ions increase the T_m value of the tertiary structure unfolding by about 7 °C compared to potassium ions. Since tertiary structure unfolding is involved in the transition under consideration, the difference, mentioned above, can be explained quantitatively by the higher stabilizing influence of Na^+ ions compared to K^+ ions.

The low-temperature transition in the 1.0 M NaCl solution closely resembles that in 0.15 M KCl, although there are some pertinent differences. In the high salt solution the melting transition is accompanied again by a decrease of the intensity of the resonances as in the low salt solution indicating the same mechanism in this case. However, in the 1.0 M NaCl solution the resonances rather abruptly disappear between 53 and 61 °C. This behavior can be understood by considering the temperature-jump results. From the temperature-jump experiments one obtains a helix lifetime of 6 ms at 61 °C. Consequently, the NMR lines will be broadened considerably at this temperature. Moreover, the equilibrium has shifted already beyond the transition point and the intensity of the resonances will have dropped accordingly. Thus, these two effects, the combination of the reduced intensity and the lifetime broadening, lead to an abrupt loss of the NMR lines in this temperature region.

Discussion

(A) *Interpretation of the NMR Spectra.* Comparison of calculated vs. experimentally observed resonance positions of the yeast $tRNA^{Gly}$ spectrum shows good agreement between the two sets of data (Table II). The standard deviation $|\delta_{obsd} - \delta_{calcd}|/20 = 0.17$ ppm including contributions from the base pairs at the ends of double helical regions. This is close to the numbers found for the spectra of *E. coli* $tRNA^{Glu}$ (Hilbers and Shulman, 1974) and yeast $tRNA^{Asp}$ (Robillard et al., 1976) demonstrating that the ring current calculations based on the cloverleaf structure provide, in a first approximation, a good model for the interpretation of tRNA spectra.

In the calculation of the spectrum of the present yeast $tRNA^{Gly}$ it was assumed as before (Shulman et al., 1973) that the acceptor arm is stacked on the TψC arm. As can be seen from base pairs 7 and 46 (from the number between the brackets), the calculations do not critically depend on this assumption, so that this structural feature cannot be tested in this case.

The main contribution to the upfield shift of base pair 1 comes from the stacking of A-70. The difference $\delta_{obsd} - \delta_{calcd} = -0.2$ ppm is not significantly different from the standard deviation of 0.17 ppm indicating that A-70 indeed stacks on base pair 1 in a regular fashion. This was also concluded from the spectrum of *E. coli* $tRNA^{Glu}$ and is compatible with the crystal structure of yeast $tRNA^{Phe}$ (Kim et al., 1974; Robertus et al., 1974).

The good agreement between the calculated and observed position of G·C-26 might be fortuitous. As has been discussed for *E. coli* $tRNA^{Glu}$ there are indications that the base between the DHU and anticodon arm is not stacked in a regular fashion between these two stems. The shift contribution indicated between the brackets (Table II) comes from G-43. Since base pair 10 is a GU combination we have no cross-check on this shift contribution.

The observed position of only one base pair, namely A·U-28, is considerably different from its calculated position. We could, however, interchange the assignments of A·U-11 and A·U-28 so that we cannot really say for which base pair the deviation exists.

The low-field resonance at −14.7 ppm which is split at high salt concentrations as well as in the presence of Mg^{2+} ions is thought to be composed of A·U-11 (or A·U-28 as has been discussed above) and a tertiary structure hydrogen-bonded proton. At the moment we have no clue as to the possible combination of bases which might generate a tertiary resonance at such a low field. In several *E. coli* tRNAs resonances have been observed at this field position. There are indications that they originate from the pairing of A-13 with thio U-8 (Kearns et al., 1974; Reid et al., 1975). Yeast $tRNA^{Gly}$, however, does not have a thio U residue in position 8.

(B) *Formation of New Structure during Melting.* The analysis of the combined NMR and temperature-jump experiments shows that there is good agreement between the kinetic parameters obtained by both methods. In a first approximation, however, the thermodynamic parameters ob-

tained from the optical experiments seem inconsistent with the NMR results. From the reaction enthalpies associated with the individual melting transitions it initially seemed likely that transition I corresponded to disrupture of the tertiary structure and the DHU stem, transition II to the anticodon and acceptor stem, and finally transition III to the TψC stem. On the other hand the interpretation of the NMR spectra indicates that during transition I the tertiary structure plus the DHU and the anticodon stems are melted out. On the basis of the latter interpretation one is forced to assume that the acceptor arm melts during the second transition and the TψC stem during the third. The reaction enthalpy obtained for the second transition is of the order of 100 kcal/mol (Table III), which is unacceptably high for the melting of a single tRNA branch. A good estimate of the melting enthalpy of the acceptor stem can be obtained from measurements on the isolated acceptor stem of *E. coli* $tRNA^{Tyr}$ (Schulz et al., 1976), the thermodynamic difference between the acceptor stem of these tRNAs being the replacement of a G·C by an A·U pair. Taking this difference into account one estimates 67 ± 7 kcal/mol for the melting enthalpy of the acceptor stem of yeast $tRNA^{Gly}$ (Borer et al., 1974). Consequently this interpretation does not agree with the interpretation of the "NMR" melting. In these considerations, however, we did not take into account the formation of the "new structure" which can be observed in the NMR spectra during the melting in the 0.15 M KCl solution. This new structure becomes apparent through the formation of the resonance at −11.0 ppm and the increase in integrated intensity when proceeding from 35 to 40 °C (Figure 1). Its formation takes place synchronously with the melting of the DHU, anticodon, and tertiary structure. Its melting above 45 °C coincides with the melting of the rest of the resonances.

The formation of this new structure can be used to explain the abnormal enthalpy values (abnormal if the NMR interpretation is followed) of the lower two melting transitions. In this model the reaction enthalpy of transition II includes contributions from the melting of both the acceptor stem and the new structure, which explains the high value of ΔH. Considering the estimate of the ΔH of the melting of the acceptor stem one calculates about 20 kcal/mol for the melting of the new structure. On the other hand the formation of the new structure yields an amount of energy which compensates in part for the energy required for the melting of the DHU, the anticodon and the tertiary structure, thus lowering ΔH observed for transition I to about 70 kcal/mol.

The new structure is formed together with the double helix of the acceptor branch during transition II. At temperatures between transition I and II it is more stable than the native tertiary structure. A further decrease of the temperature, however, increases the stability of the native structure including the intact DHU and anticodon arms. The NMR spectra demonstrate that in this situation the noncloverleaf base pairs of the new structure have to be disrupted again. As an intermediate conformation it is more stable than intermediates derived from the cloverleaf merely by melting some regions. The feature of having noncloverleaf base pairs is similar to the denatured conformations, which have been reported for some tRNAs (e.g., Lindahl et al., 1966). The main difference, however, is that the denatured conformers known from the literature are stable at low temperatures, whereas the new structure, reported here, occurs as an intermediate state during the complete thermal denaturation of the native conformation.

(C) *Thermodynamic and Kinetic Parameters.* The reaction enthalpies of the individual melting transitions are given in Table III. The enthalpy values of the lowest two transitions have already been discussed in the preceding section. The melting of the TψC stem (transition III) is reasonably isolated from the melting of the rest of the molecule and the enthalpy of 55 kcal/mol compares nicely with a predicted value of 52 kcal/mol calculated on the basis of the empirical thermodynamic parameters given by Gralla and Crothers (1973) and by Borer et al. (1974). Moreover, it is interesting to compare its thermodynamic and kinetic parameters with those of the isolated TψC hairpin of yeast $tRNA^{Asp}$ which also contains five G·C pairs and an identical loop sequence except for G-54 which is converted to an A in yeast $tRNA^{Asp}$ (Coutts et al., 1974). The reaction enthalpy of 62 kcal/mol at the T_m (79 °C) agrees within experimental accuracy with the value of 55 kcal/mol measured in yeast $tRNA^{Gly}$. In addition in both systems the relaxation times are near 30 μs at 76 °C. For the TψC hairpin of yeast $tRNA^{Asp}$ the dissociation activation enthalpy and the melting enthalpy were found to be almost identical. Since the thermodynamic and kinetic parameters of both, the TψC branch in yeast $tRNA^{Gly}$ and the isolated TψC hairpin of yeast $tRNA^{Asp}$, are so similar we assumed the dissociation activation enthalpy of the TψC arm in yeast $tRNA^{Gly}$ to be equivalent to its melting enthalpy also (cf. Results, section D).

Yeast $tRNA^{Gly}$ is the third tRNA molecule for which the melting has been studied in such detail, the other two being yeast $tRNA^{Phe}$ (Riesner et al., 1973) and *E. coli* $tRNA^{fMet}$ (Crothers et al., 1974). The tertiary structure is found to be the least stable part of the molecule.

Evidence is mounting that during protein synthesis the interaction between the DHU loop and the TψC loop is disrupted. According to the crystal structure (Kim et al., 1974; Robertus et al., 1974), chemical modification studies (Cramer, 1971), and oligonucleotide binding studies (Uhlenbeck et al., 1970) the TψC sequence is shielded from the outside by this loop–loop interaction. Yet these residues are involved in the binding of the tRNA molecule to the ribosome (Richter et al., 1974). In line with this the thermodynamic studies carried out so far, although conducted under nonphysiological conditions, clearly indicated that the tertiary structure belongs to the weakest part of the tRNA molecules under investigation. Recent enzymatic and thermodynamic experiments indicate that a weakening of the loop–loop interaction may be induced by the biogenic amine cadaverine, and that only some of the tertiary structure interactions are involved (Wildenauer et al., 1974).

As in the present study the melting of the tertiary structure is often coupled to the melting of the DHU arm (Crothers et al., 1974; Hilbers and Shulman, 1974). Thermodynamically this can be expected for yeast $tRNA^{Gly}$ since the DHU stem containing two A·U, one A·ψ, and one G·U base pairs is rather unstable. The significance for the understanding of the mechanism of protein synthesis, however, is not completely clear.

Evidently the TψC loop would be accessible after opening of the tertiary structure and DHU stem, but this does not implicate that both transitions are a general prerequisite for the interaction with ribosomal factors and ribosomes. In yeast $tRNA^{Phe}$ the DHU stem is one of the most stable parts of the molecule (Römer et al., 1969) and its dissociation during ribosome binding seems unlikely.

References

Borer, N. P., Dengler, B., Tinoco, I., and Uhlenbeck, O. C. (1974), *J. Mol. Biol. 86,* 843.

Coutts, S. M., Gangloff, J., and Dirheimer, G. (1974), *Biochemistry 13,* 3938.

Cramer, F. (1971), *Prog. Nucleic Acid Res. Mol. Biol. 2,* 391.

Crothers, D. M., Cole, P. E., Hilbers, C. W., and Shulman, R. G. (1974), *J. Mol. Biol. 87,* 63.

Crothers, D. M., Hilbers, C. W., and Shulman, R. G. (1973), *Proc. Natl. Acad. Sci. U.S.A. 70,* 2899.

Eigen, M., and de Maeyer, L. (1963), *Tech. Org. Chem. 8.*

Gralla, J., and Crothers, D. M. (1973), *J. Mol. Biol. 73,* 497.

Hilbers, C. W., and Shulman, R. G. (1974), *Proc. Natl. Acad. Sci. U.S.A. 71,* 3239.

Kim, S. H., Suddath, F. L., Quigley, G. J., McPherson, A., Sussman, J. L., Wang, A. H. J., Seeman, N. C., and Rich, A. (1974), *Science 185,* 435.

Lightfoot, D. R., Wong, K. L., Kearns, D. R., Reid, B. R., and Shulman, R. G. (1973), *J. Mol. Biol. 78,* 71.

Lindahl, T., Adams, A., and Fresco, J. R. (1966), *Proc. Natl. Acad. Sci. U.S.A. 55,* 941.

Reid, B. R., Ribeiro, N. S., Gould, G., Robillard, G. T., Hilbers, C. W., and Shulman, R. G. (1975), *Proc. Natl. Acad. Sci. U.S.A. 72,* 2049.

Richter, D., Erdmann, V. A., and Sprinzl, M. (1974), *Proc. Natl. Acad. Sci. U.S.A. 71,* 3226.

Riesner, D., Maass, G., Thiebe, R., Phillipsen, P., and Zachau, H. G. (1973), *Eur. J. Biochem. 36,* 76.

Robertus, J. D., Ladner, J. E., Finch, J. T., Rhodes, D., Brown, R. S., Clarck, B. F. C., and Klug, A. (1974), *Nature (London) 250,* 546.

Robillard, G. T., Hilbers, C. W., Reid, B. R., Gangloff, J., Dirheimer, G., and Shulman, R. G. (1976), *Biochemistry,* following paper in this journal.

Römer, R., and Riesner, D. (1973), in Physico-Chemical Properties of Nucleic Acids, Duchesne, J., Ed., London and New York, Academic Press.

Römer, R., Riesner, D., Maass, G., Wintermeyer, W., Thiebe, R., and Zachau, H. G. (1969), *FEBS Lett. 5,* 15.

Schulz, E., Riesner, D., Maass, G., and Gross, H. (1976), manuscript in preparation.

Shulman, R. G., Hilbers, C. W., Kearns, D. R., Reid, B. R., and Wong, Y. P. (1973), *J. Mol. Biol. 78,* 57.

Uhlenbeck, O. C., Baller, J., and Doty, P. (1970), *Nature (London) 225,* 508.

Urbanke, C., Römer, R., and Maass, G. (1975), *Eur. J. Biochem. 55,* 439.

Wildenauer, D., Gross, H. J., and Riesner, D. (1974), *Nucleic Acids Res. 1,* 1165.

Wong, K., and Kearns, D. R. (1974), *Nature (London) 252,* 738.

Yoshida, M. (1973), *Biochem. Biophys. Res. Commun. 50,* 779.